

The reduction behavior of the Cu ion species exchanged into Y zeolite during the thermovacuum treatment

Haijun Chen^a, Masaya Matsuoka^a, Jinlong Zhang^b, Masakazu Anpo^{a,*}

^a Department of Applied Chemistry, Graduate School of Engineering, Osaka Prefecture University, 1-1 Gakuen-cho Sakai, Osaka 599-8531, Japan

^b Institute of Fine Chemicals, East China University of Science and Technology, 130 Meilong Road, Shanghai 200237, People's Republic of China

Received 17 June 2004; revised 21 August 2004; accepted 23 August 2004

Available online 25 September 2004

Abstract

The changes observed in the valence state and local structure of the Cu species present in the Cu ion-exchanged Y zeolite during thermovacuum treatment have been investigated by ESR and photoluminescence techniques. Especially, the reduction behavior of the Cu(II) monomers and Cu(II) dimers which exist in the Y zeolite has been studied according to the changes seen in their ESR spectra during such thermovacuum treatment. Moreover, the mechanism for the formation of the Cu(I) monomers and dimers after thermovacuum treatment has been proposed based on investigations of the deconvoluted photoluminescence spectra.

© 2004 Elsevier Inc. All rights reserved.

Keywords: Y zeolite; Cu(I); Reduction of Cu(II); Monomer; Dimer

1. Introduction

Many studies have been devoted to the identification of different types of Cu species present in zeolites and to revealing their role during the catalytic reactions and procedures, especially since the discovery of the high activity of overexchanged Cu-ZSM5 for the decomposition of NO by Iwamoto et al. [1–6]. Moreover, on the basis of TPR (temperature-programmed reduction) and TPD (temperature-programmed desorption) analyses, Iglesia and co-workers [2] have determined the content of the isolated Cu(II) monomers and oxygen-bridged Cu(II) dimers ($\text{Cu}^{2+}-\text{O}^{2-}-\text{Cu}^{2+}$) in Cu-ZSM5 and found that the turnover rates of the decomposition reaction of NO (normalized per Cu dimer) were nearly independent of the Cu content while the Cu dimers were considered as the active Cu species in the NO decomposition redox cycles. Furthermore, the Cu(I)

dimers (Cu^+-Cu^+) were proposed to be responsible for the catalytic decomposition reaction of NO based on analyses of IR [1,6], XAFS (X-ray absorption fine structure) [7], and DFT (density-functional theory) [8]. However, until now, few works have been conducted on exploring both the reduction behavior of the Cu(II) dimers and the formation of Cu(I) dimers despite much attention into the redox chemistry of copper in zeolites. Although there have been a few reports on Cu(II) dimers and Cu(I) dimers [9,10], neither the relationship between the Cu ion monomers and dimers nor the reduction process of the various Cu(I) species have been clarified.

Taking into account the fact that Cu dimers play an important role in the NO decomposition reaction, in the present paper, the effects of Cu loading and thermovacuum treatment of Cu–Y on the Cu(II) dimers/Cu(II) monomers ratio have been quantitatively determined by detailed deconvolution analysis of the ESR signals due to the Cu(II) ions. Furthermore, the presence of several kinds of Cu(I) species have been elucidated by the quantitative deconvolution of the photoluminescence spectra and the effect of the Cu loadings as well as the evacuation temperature on the relative

* Corresponding author. Fax: +81-72-254-9910.

E-mail addresses: chenhj@ok.chem.osakafu-u.ac.jp (H. Chen), matsumac@ok.chem.osakafu-u.ac.jp (M. Matsuoka), jlzhang@ecust.ac.cn (J. Zhang), anpo@ok.chem.osakafu-u.ac.jp (M. Anpo).

amount of the various Cu(I) species within the Y zeolite have also been investigated in detail. Special attention has been focused on the reduction mechanism of Cu(II) species within the Y zeolite, especially on the changes in the coordination symmetry of the Cu species during thermovacuum treatment.

2. Experimental

The Na–Y zeolite (Tosoh Corp.) with a Si/Al ratio of 2.8 was used as the parent zeolite. The Na–Y zeolite was ion-exchanged with a NH_3 buffer aqueous solution (2 M $\text{NH}_3/0.05$ M NH_4NO_3) for 24 h followed by calcination treatment in air at 773 K to obtain an H–Y zeolite. Cu(I)–Y zeolites with various Cu loadings were prepared by a combination of an ion-exchange method and thermovacuum treatment at various temperatures, as follows: The H–Y zeolite was exchanged with a $\text{Cu}(\text{NO}_3)_2$ aqueous solution having different pH values at 298 K for 24 h. The amount of ion-exchanged Cu ions was controlled by the concentration and the pH of the $\text{Cu}(\text{NO}_3)_2$ aqueous solution, the pH being adjusted by changing the ratio of $\text{NH}_3/\text{NH}_4\text{NO}_3$ concentration in the solution. The increase of the pH of the $\text{Cu}(\text{NO}_3)_2$ aqueous solution led to a color change of the solution into dark blue while no formation of a precipitate was observed. After the ion exchange, the samples were washed with distilled water and then dried in air at 373 K for 24 h. Finally, the samples were degassed at different temperatures and the Cu(I)–Y catalysts were prepared by an autoreduction reaction. The copper loading of the Cu(II)–Y zeolite samples was determined by an atomic absorption flame emission spectrophotometer (Shimadzu AA-6400F). A quartz cell with window and furnace sections, having a volume of ca. 50 cm^3 , was connected to a vacuum system for pretreatment and used for the in situ measurements of the spectra. Both the ESR and the photoluminescence spectra of the samples were recorded at 77 K with a JES-RE2X spectrometer operating in the X-band mode and a Spex Fluorolog II spectrofluorimeter, respectively. The obtained spectra were deconvoluted by a computerization data analyzing system.

3. Results and discussion

The copper contents of the Cu(II)–Y samples increased with an increase in the pH values of the $\text{Cu}(\text{NO}_3)_2$ solution, as shown in Fig. 1. When the pH value of the $\text{Cu}(\text{NO}_3)_2$ solution is high, the copper ions were considered to be exchanged at the Brönsted acid sites of the Y zeolite in the form of $[\text{Cu}^{2+}(\text{OH})^-]^{+}$ [15] or ammonia-coordinated $[\text{Cu}^{2+}(\text{OH})^-]^{+}$ complexes. Also, considering that the divalent Cu(II) ions, which compensate two Brönsted acid sites, are the main Cu(II) moiety in the low pH, it is plausible that the copper content increases with an increase in the pH

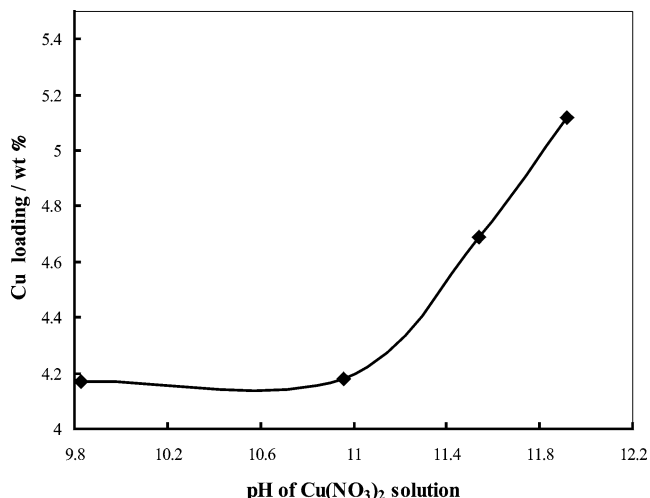
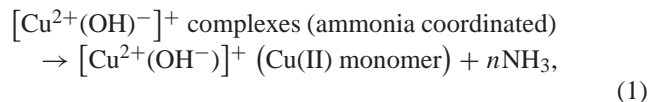


Fig. 1. The effect of the pH of the $\text{Cu}(\text{NO}_3)_2$ solution (0.08 M) on the Cu(II) loading of the Cu(II)–Y zeolites.

of the $\text{Cu}(\text{NO}_3)_2$ solution since monovalent $[\text{Cu}^{2+}(\text{OH})^-]^{+}$ or ammonia-coordinated $[\text{Cu}^{2+}(\text{OH})^-]^{+}$ complexes become dominant at high pH levels. However, ion-exchange procedures repeated three times under optimum exchange conditions (0.08 M, pH 11.9) led to only a slight increase in the Cu/Al ratios from 0.203 to 0.235, showing that not all the ion-exchange sites can be displaced by the Cu ions in the Y zeolite with such a low Si/Al ratio.

The ESR spectrum of the Cu–Y zeolite evacuated at 673 K has been well deconvoluted into two kinds of spectral components, i.e., an isotropic component ($g_{\text{iso}} = 2.17\text{--}2.18$) and an anisotropic component ($g_{//} = 2.33\text{--}2.31$, $A_{//} = 165\text{--}155$ G), which can be attributed to the spin–spin-interacted Cu(II) ions (Cu(II) dimers) [14–16] and isolated Cu(II) ions with square pyramidal coordination [11,16–18], respectively, as shown in Fig. 2. Moreover, the signal intensities of these two Cu(II) species were determined by the integral area of the corresponding deconvoluted spectrum. It should be noted that ESR signal due to $\Delta m_s = 2$ transition of Cu(II) dimers was also detected in the $g = 4$ region, and a good relationship was observed between the integral intensity of the ESR signal appearing in the $g = 4$ region and that of the corresponding isotropic signal in the $g = 2$ region [19,20]. These results also show that the isotropic ESR signal observed around the $g = 2$ region can be assigned to the spin–spin-interacted Cu(II) ions (Cu(II) dimers).

Fig. 3 shows the effect of the Cu(II) loading on the molar ratio of the Cu(II) monomers and dimers within the Cu–Y zeolites evacuated at 673 K for 1 h. At this stage, the Cu(II) monomers and Cu(II) dimers are formed through the desorption of NH_3 and H_2O following the mechanism indicated below [12,21,22]:



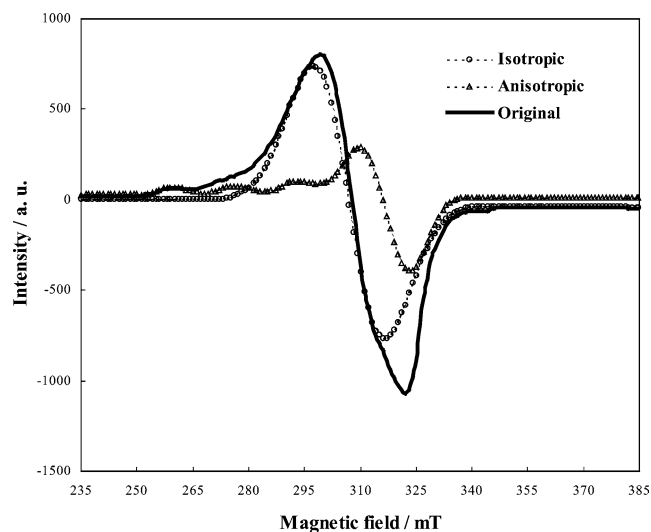


Fig. 2. The ESR spectrum of the Cu–Y zeolite (Cu/Al = 0.165) evacuated at 673 K for 1 h and their deconvoluted spectra.

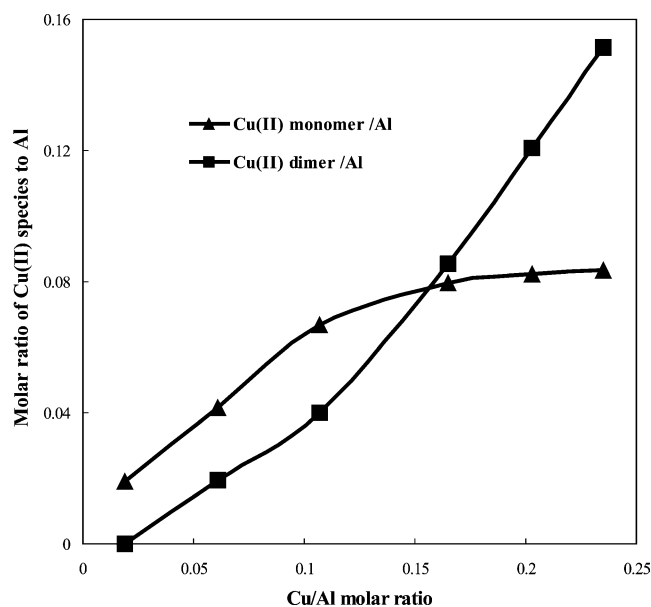
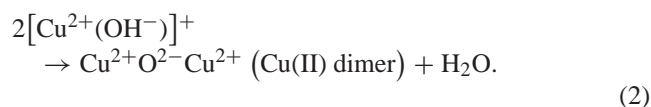


Fig. 3. The effect of the Cu(II) loading on the molar ratio of the Cu(II) monomers and Cu(II) dimers to the framework Al, as determined by the integral area of the deconvoluted ESR spectra observed for Cu–Y zeolites evacuated at 673 K for 1 h.



As shown in Fig. 3, the fraction of Cu(II) dimers increases almost linearly with an increase in the Cu/Al ratio, while that of the Cu(II) monomers reaches a plateau at around 0.08 (Cu(II) monomer/Al ratio), showing a good agreement with the result observed with Cu–ZSM5, as reported by Iglesia and co-workers [2]. These results suggest that the Cu(II) ions are exchanged at the closely neighboring pair sites of the Brönsted Al–OH–Si groups, predominantly in the case of low Cu(II) content, while the Cu(II) ions are exchanged at

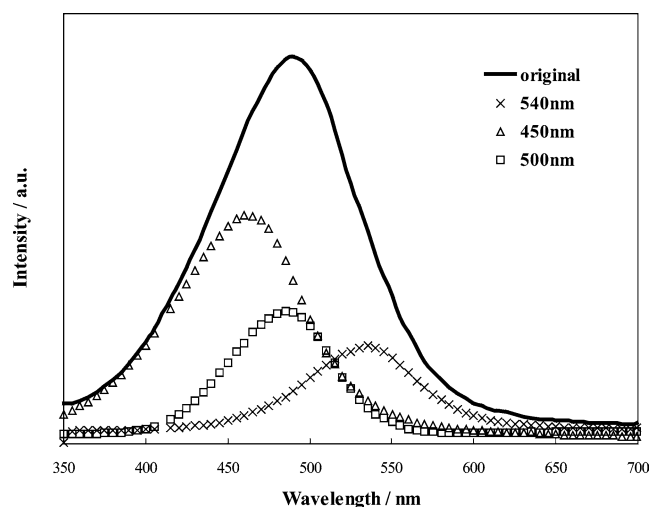


Fig. 4. The deconvoluted spectra of the photoluminescence observed for the Cu–Y zeolite (Cu/Al = 0.165) evacuated at 1073 K.

the pair sites of the Brönsted Al–OH–Si groups separated by a relatively long distance to form Cu(II) dimers (Cu(II)–O–Cu(II)) in the case of high Cu(II) content.

High-temperature evacuation of the Cu(II)–Y zeolites at 1073 K led to the appearance of characteristic photoluminescence at around 400–600 nm under photoexcitation at around 285 nm, indicating that the reduction of the Cu(II) ions to Cu(I) ions occurs. The photoluminescence spectra, due to Cu(I) ions, have been deconvoluted into three main bands at around 450, 500, and 540 nm, respectively, as shown in Fig. 4. All of these deconvoluted photoluminescence components of Cu(I) are similar to those reported in previous literature [13]. Dedecek et al. [14] have reported that the relative intensities of these three photoluminescence bands vary depending on the Si/Al ratio of the Y zeolites. According to previous studies on the photoluminescence of Cu(I) ions [23–27], the photoluminescence bands at 450 and 540 nm can be assigned to the radiative deactivation process of the photoexcited two-coordination Cu(I) monomer ($3d^94s^1 \rightarrow 3d^{10}$) and Cu(I)–Cu(I) dimer ($4s\sigma \rightarrow 3d\sigma^*$), respectively. It has also been reported that the emission bands at around 500 nm are attributed to the radiative deactivation process of the photoexcited planar three-coordinated Cu(I) monomer ($3d^94s^1 \rightarrow 3d^{10}$) [11]. Based on these assignments, it can be concluded that three kinds of Cu(I) moieties with different coordination spheres are present in Cu(I)–Y zeolites evacuated at high temperatures.

As shown in Fig. 5, Cu(II) dimers are more easily reduced by the thermovacuum treatment than Cu(I) monomers. Moreover, the intensity of the photoluminescence spectra due to the two-coordination Cu(I) monomers as well as Cu(I)–Cu(I) dimers is seen to increase with a decrease in the intensity of the ESR signals due to the Cu(II) monomers and Cu(II) dimers, when the degassing temperature of the original Cu(II)–Y sample was increased. These results clearly suggest that the Cu(II) monomers and dimers are reduced into Cu(I) monomers and dimers. The intensity of the pho-

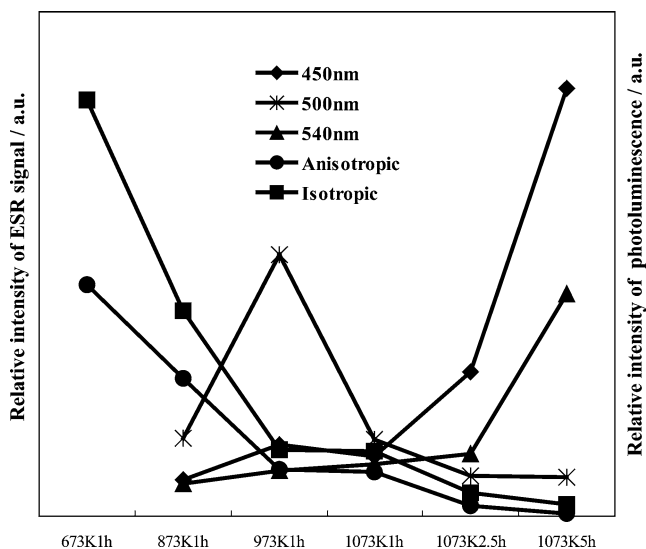


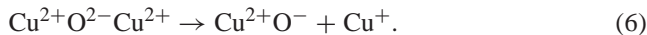
Fig. 5. The effect of the evacuation temperature as well as evacuation time of the Cu(II)-Y (Cu/Al = 0.203) sample on the relative intensity of the ESR signal attributed to Cu(II), and the relative intensity of photoluminescence attributed to Cu(I).

toluminescence spectrum due to three-coordination Cu(I) monomers ($\lambda = 500$ nm) reaches a maximum at 973 K and then decreases by further evacuation treatment, suggesting that the three-coordination Cu(I) monomers are not energetically favorable under high-temperature treatment and are converted into two-coordination Cu(I) monomers or Cu(I) dimers.

Based on these results, the mechanism of the reduction of Cu ions during the thermovacuum treatment has been proposed, as shown below. Cu(II) monomers are considered to be reduced according to the mechanism proposed by Larsen et al. [28] under degassing treatment at temperatures below 973 K:



At the same time, the Cu(II) dimers are also partially reduced to Cu(I) ions with the formation of Cu^{2+}O^- , as suggested in Eq. (6). Both the intensity of the ESR signal due to Cu(II) monomers and the dimers decrease quickly due to the formation of Cu(I) ions and the ESR silent Cu^{2+}O^- [28],



Further thermovacuum treatment at 1073 K caused the ESR silent Cu^{2+}O^- species to be reduced to Cu(I) ions [Eq. (7)], while the three-coordination Cu(I) monomers were converted into two-coordination Cu(I) monomers or Cu(I) dimers. These reduction of the ESR silent Cu^{2+}O^- species as well as the conversion of the unstable three-coordination Cu(I) monomers into other kinds of Cu(I) species led to a marked growth in the photoluminescence bands at 450 nm and 540 nm at 1073 K, as shown in Fig. 5,

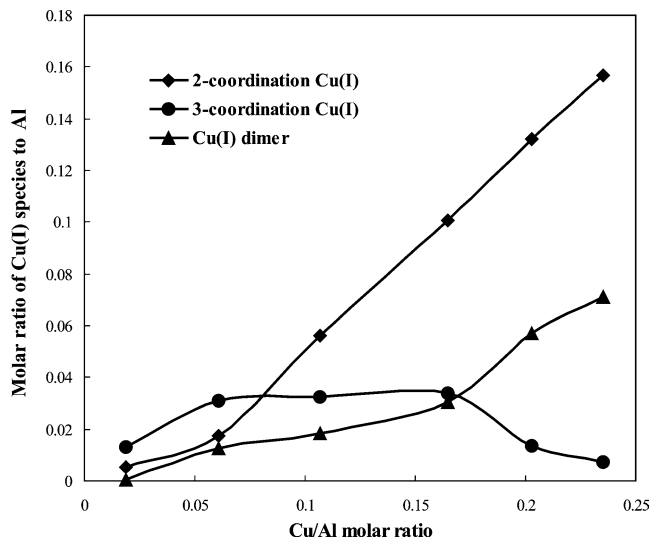


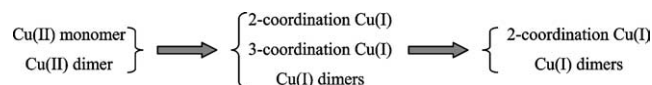
Fig. 6. The effect of Cu(II) loading on the molar ratio of Cu(I) species to the framework Al determined by the intensities of the deconvoluted photoluminescence spectra of Cu-Y zeolites evacuated at 1073 K.

Fig. 6 shows the effect of the Cu(II) loading on the molar ratio of the two kinds of Cu(I) monomers and dimers to the framework Al, determined by the intensities of the deconvoluted photoluminescence spectra of the Cu-Y zeolites evacuated at 1073 K. Here, the evacuation time at 1073 K has been adjusted so that a maximum photoluminescence can be observed.

It was found that the three-coordination Cu(I) monomers are the predominant species after the reduction of the Cu(II) ions in the Cu-Y zeolite with a low Cu(II) loading. However, when the Cu(II)/Al ratio exceeds 0.16, the amount of three-coordination Cu(I) monomers decreases, indicating that these monomers are converted to two-coordination Cu(I) monomers or Cu(I) dimers in the case of a high Cu(II) loading. On the other hand, Cu(I) monomers are the predominant species even for Cu-Y zeolites with high Cu loadings, where Cu(II) dimers are the main species before reduction, as shown in Fig. 3. This suggests that at least some part of the Cu(II) dimers were reduced preferably to Cu(I) monomers than directly to Cu(I) dimers, showing a good agreement with the mechanism proposed in Eq. (6). Furthermore, the amount of Cu(I) dimers increased with an increase in the two-coordination Cu(I) monomer, as shown in Fig. 6, suggesting that a large amount of Cu(I) dimers was formed through the interaction between the two-coordination Cu(I) monomers which exist in near proximity to each other within the Cu-Y zeolite:



The reduction route of the Cu(II) species present in Cu-Y zeolite can, thus, be proposed as shown in Scheme 1. Cu(II) monomers and dimers within the Cu-Y zeolite would be reduced to two-coordination Cu(I) monomers, three-coordination Cu(I) monomers, and Cu(I) dimers after thermovacuum treatment. The three-coordination Cu(I)



Scheme 1. The reduction of Cu(II) ions in the Y zeolite.

monomers are converted into two-coordination Cu(I) monomers or Cu(I) dimers under high-temperature treatment or in the case of high Cu(II) loadings. The increased amount of two-coordination Cu(I) monomers which exist in near proximity to each other on the Cu–Y zeolites is considered to lead to the formation of the Cu(I) dimers.

4. Conclusions

Not all of the ion exchange sites are seen to be exchanged by Cu ions in the Y zeolite with a low Si/Al ratio. During the course of ion exchange, the Cu ions are, at first, exchanged as Cu(II) monomers at closely neighboring pair sites of the Brönsted Al–OH–Si groups, then the Cu ions are exchanged as Cu(II) dimers (Cu(II)–O–Cu(II)) at those pair sites separated by a long distance, in accordance with the increase in Cu content.

Cu(II) monomers and dimers formed within the Cu–Y zeolite are reduced to two-coordination Cu(I) monomers and three-coordination Cu(I) monomers as well as Cu(I) dimers after thermovacuum treatment. Moreover, three-coordination Cu(I) monomers are converted into two-coordination Cu(I) monomers or Cu(I) dimers under high-temperature treatment or in the case of high Cu(II) loadings. Some parts of the Cu(II) dimers can be reduced to Cu(I) monomers and an increase in the two-coordination Cu(I) monomers which exist in close proximity to each other within the Cu–Y zeolites led to the formation of Cu(I) dimers.

References

[1] M. Iwamoto, H. Furukawa, Y. Mine, F. Uemura, S.I. Mikuriya, S. Kagawa, *J. Chem. Soc., Chem. Commun.* (1986) 1272.

- [2] P. Da Costa, B. Moden, G.D. Meitzner, D.K. Lee, E. Iglesia, *Phys. Chem. Chem. Phys.* 4 (2002) 4590.
- [3] E. Giamello, D. Murphy, G. Magnacca, C. Morterra, Y. Shioya, T. Nomura, M. Anpo, *J. Catal.* 136 (1992) 510.
- [4] M. Anpo, M. Che, *Adv. Catal.* 44 (2000) 119.
- [5] M. Matsuoka, M. Anpo, *J. Photochem. Photobiol. C* 3 (2003) 225.
- [6] M. Iwamoto, H. Yahiro, N. Mizuno, W.X. Zhang, Y. Mine, H. Furukawa, S. Kagawa, *J. Phys. Chem.* 96 (1992) 9360.
- [7] M.H. Groothaert, J.A. van Bokhoven, A.A. Battiston, B.M. Weckhuysen, R.A. Schoonheydt, *J. Am. Chem. Soc.* 125 (2003) 7629.
- [8] B.R. Goodman, W.F. Schneider, K.C. Hass, J.B. Adams, *Catal. Lett.* 56 (1998) 183.
- [9] G.T. Palomino, P. Fisticaro, S. Bordiga, A. Zecchina, E. Giamello, C. Lamberti, *J. Phys. Chem. B* 104 (2000) 4064.
- [10] J. Sarkany, J.L. D'Itri, W.M.H. Sachtler, *Catal. Lett.* 16 (1992) 241.
- [11] M. Matsuoka, W.S. Ju, K. Takahashi, H. Yamashita, M. Anpo, *J. Phys. Chem. B* 104 (2000) 4911.
- [12] M. Iwamoto, H. Yahiro, N. Mizuno, Y.W.X. Zhang, Y. Mine, S. Kagawa, *J. Phys. Chem.* 96 (1992) 9360.
- [13] G. Spoto, A. Zecchina, S. Bordiga, G. Ricchiardi, G. Martra, *Appl. Catal. B* 3 (1994) 151.
- [14] J. Dedecek, Z. Sobalik, Z. Tvaruzkova, D. Kaucky, B. Wichterlova, *J. Phys. Chem.* 99 (1995) 16327.
- [15] M. Iwamoto, H. Yahiro, Y. Torikai, T. Yoshioka, N. Mizumo, *Chem. Lett.* (1990) 1967.
- [16] J. Goslar, A.B. Wieckowski, *J. Solid State Chem.* 56 (1985) 101.
- [17] R.G. Herman, D.R. Flentge, *J. Phys. Chem.* 82 (1978) 720.
- [18] J.C. Conesa, J. Soria, *J. Chem. Soc., Faraday Trans.* 75 (1979) 406.
- [19] C.C. Chao, J.H. Lunsford, *J. Chem. Phys.* 57 (1974) 2890.
- [20] S. Schlick, M.G. Alonso-Amigo, S.S. Eaton, *J. Phys. Chem.* 93 (1989) 7906.
- [21] M. Iwamoto, H. Yahiro, Y. Mine, S. Kagawa, *Chem. Lett.* (1989) 213.
- [22] M. Iwamoto, H. Yahiro, K. Tanda, N. Mizuno, Y. Mine, S. Kagawa, *J. Phys. Chem.* 95 (1991) 3727.
- [23] J.D. Barrie, B. Dunn, *J. Phys. Chem.* 93 (1989) 3958.
- [24] D.H. Strome, K. Klier, *J. Phys. Chem.* 84 (1980) 981.
- [25] M. Anpo, M. Matsuoka, Y. Shioya, H. Yamashita, E. Giamello, C. Morterra, M. Che, H.H. Patterson, S. Webber, S. Ouellette, M.A. Fox, *J. Phys. Chem.* 98 (1994) 5744.
- [26] M. Anpo, T. Nomura, Y. Shioya, M. Che, D. Murphy, E. Murphy, in: L. Guzzi, et al. (Eds.), *Proc. 10th Int. Congr. Catal., Akademiai Kiado, Budapest*, 1993, p. 2155.
- [27] H. Yamashita, M. Matsuoka, K. Tsuji, Y. Shioya, M. Anpo, M. Che, *J. Phys. Chem.* 100 (1996) 397.
- [28] S.C. Larsen, A. Aylor, A. Bell, J.A. Reimer, *J. Phys. Chem.* 98 (1994) 11533.